0273-2289/1559–0291 (Online)/07/136–140/817–834/$30.00

Hybrid Neural Network Model of an Industrial Ethanol Fermentation Process Considering the Effect of Temperature

Ivana C. C. Mantovanelli,[1] Elmer Ccopa Rivera,[2] Aline C. da Costa,*[,2] and Rubens Maciel Filho[2]

[1]Department of Biotechnological Processes; and [2]Department of Chemical Processes, School of Chemical Engineering—UNICAMP, Cidade Universitária "Zeferino Vaz"—Caixa Postal 6066—CEP 13083-970–Campinas–SP—Brasil, E-mail: accosta@feq.unicamp.br

Abstract

In this work a procedure for the development of a robust mathematical model for an industrial alcoholic fermentation process was evaluated. The proposed model is a hybrid neural model, which combines mass and energy balance equations with functional link networks to describe the kinetics. These networks have been shown to have a good nonlinear approximation capability, although the estimation of its weights is linear. The proposed model considers the effect of temperature on the kinetics and has the neural network weights reestimated always so that a change in operational conditions occurs. This allow to follow the system behavior when changes in operating conditions occur.

Index Entries: Alcoholic fermentation; functional link networks; kinetic parameters estimation; mathematical modeling; process simulation; bioreactors.

Introduction

A potential substitute for petroleum in Brazil is biomass, particularly sugar cane. The sugar cane industry is the largest alternative commercial energy production program in the world with ethanol and the almost complete use of sugar cane bagasse as fuel. Although the bioethanol production is running for several years it is clear that improvements are required to increase the process performance. The influence of temperature in the kinetics is a very important factor in the alcoholic fermentation process. It is difficult to support a constant temperature during large-scale alcoholic fermentation and variations in temperature affects productivity through changes in kinetics as well as in microorganism lifetime. The temperature in a typical industrial fermentor varies from 33.5°C (during the night) to

*Author to whom all correspondence and reprint requests should be addressed.

35°C (at the end of the day) owing to fluctuations in the cooling water temperature. In plants with poor temperature control the temperature in the fermentor goes up to 40°C. Thus, an accurate mathematical model must take the influence of temperature into account. Also, changes in operational conditions and fluctuations in raw material composition, both very common in alcoholic fermentation plants, results in kinetic changes and affects yield and productivity.

Owing to the difficulties described above, the main difficulty in model-based techniques for definition of operational strategies, control, and optimization for the ethanol production process is the problem of obtaining an accurate model. Thus, in this work a procedure for the development of robust mathematical models for the alcoholic fermentation process is evaluated. The objective is to obtain a model to be used as a simulator, making simpler not only the development and implementation of new control and optimization techniques, but also retuning of existing controllers as well as finding out new optimal operational conditions when operational changes occur.

In the last years, many studies of the mathematical modeling of alcoholic fermentation process have been performed *(1,2)*. However, although temperature has an important influence on this process, there are very few works in the literature considering the effect of temperature on the kinetic parameters. Among them are the works of Atala et al. *(3)* and Aldiguier et al. *(4)*. However, Aldiguier et al. *(4)* determined different values for kinetic parameters in different temperatures, but did not determine a temperature function to describe the kinetic parameters. Although phenomenological mathematical models provide understanding about the process, practical experience shows that they are only valid for the specific conditions in which they were determined. When there are changes in operational conditions, the model kinetic parameters have to be reestimated. The frequent reestimation, mainly when the parameters are described as functions of temperature, is difficult and time-consuming because of nonlinearities, great number of parameters, and interactions among them.

One way to deal with this problem is to use hybrid neural models *(5,6)*. As was demonstrated by Psichogious and Ungar *(7)*, it is simple to propose a bioreactor mathematical model through application of mass balances for the process variables. The really difficult part is the mathematical representation of the kinetics. A cell is a complex organism wherein thousands of enzyme-catalyzed reactions take place. The kinetic rates are most often poorly understood nonlinear functions; whereas the corresponding parameters are in general time-varying *(8)*. Literature presents a great number of approximate kinetic models, which take different factors into account, and the proper choice of the mathematical description of these expressions is object of discussion in many works *(2,3,9,10)*. Thus, hybrid neural models are suitable to model biotechnological processes, as they combine mass and energy balance equations with neural networks, which represent the unknown kinetics *(11)*. In this work a hybrid neural model is proposed to

model an industrial alcoholic fermentation process. The specific growth rate is described by a functional link network (FLN) *(12)*. These networks have been shown to have a good nonlinear approximation capability, although the estimation of its weights is linear. Because of this linear estimation, the FLNs training is rapid, requires low computational effort, and convergence is guaranteed, so that it has a large potential for online control and optimization implementations *(6)*.

Industrial Alcoholic Fermentation Process—Phenomenological Model

The alcoholic fermentation process to be modeled is illustrated in Fig. 1. This is an existing plant, designed using the procedure of Andrietta and Maugeri *(13)* to a maximum production of 320 m^3 of anhydrous ethanol/d. The system is a typical large-scale industrial process made up of five continuous-stirred tank reactors attached in series and operating with cell recycle. Each reactor has an external heat exchanger to keep the temperature constant at an ideal level for the fermentation process. The feedstock, a mixture made up of sugar cane molasses and syrup and sources of nitrogen and mineral salts, is converted into ethanol by a fermentation process carried out using the yeast *Saccharomyces cerevisiae*. A set of centrifuges splits the outlet-fermented product into two phases. The light phase (F_V) is sent to a distillation tower in which the alcohol is finally obtained. The heavy phase is mixed with acid and diluted with water (flow rate F_a) before being recycled (flow rate F_R) to the first reactor. F_S (m^3/h) is the flow rate of the cell purge stream, used to permit cell renovation and the withdrawal of secondary products accumulated into the fermentor. These process-operating conditions are real conditions of typical industrial distilleries in Brazil.

The mass and energy balances for the five fermentors are:
Global mass balance in *i*th fermentor:

$$\frac{dV_i}{dt} = \frac{F_{i-1} \times \rho_{i-1}}{\rho_i} - F_i \tag{1}$$

Substrate balance in *i*th fermentor:

$$\frac{d(S_i V_i)}{dt} = F_{i-1} S_{i-1} - F_i S_i - V_i X_i \frac{1}{Y_{X/S}} \mu_i \tag{2}$$

Product balance in *i*th fermentor:

$$\frac{d(P_i V_i)}{dt} = F_{i-1} P_{i-1} - F_i P_i + V_i X_i \frac{Y_{P/S}}{Y_{X/S}} \mu_i \tag{3}$$

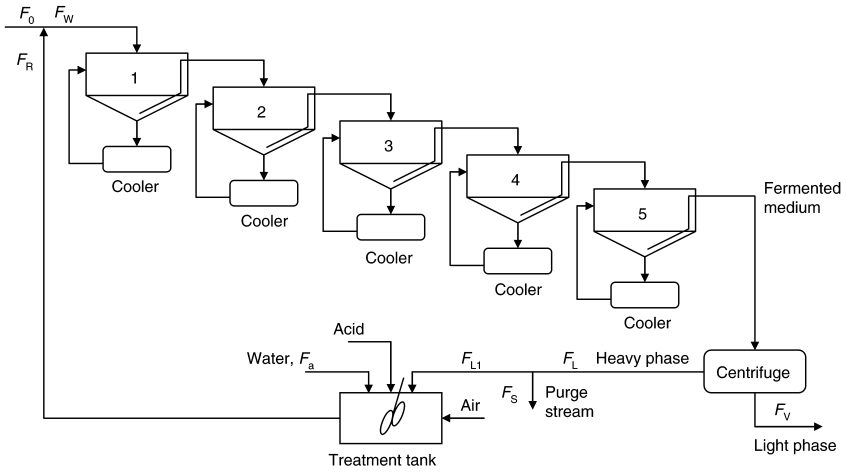

Fig. 1. Schematic illustration of an industrial plant for ethanol production.

Biomass balance in *i*th fermentor:

$$\frac{d(X_i V_i)}{dt} = F_{i-1}X_{i-1} - F_i X_i + V_i X_i \mu_i \tag{4}$$

Energy balance in *i*th fermentor:

$$\frac{d(V_i T_i)}{dt} = F_{i-1}T_{i-1} - F_i T_i + F_i(T_{Ci} - T_i) + \frac{V\Delta H X_i}{\rho_i Cp_i Y_{X/S}}\mu_i \tag{5}$$

Energy balances for the reagent fluid in *i*th heat exchanger:

$$\frac{d(T_{Ci})}{dt} = F_{Ci}(T_i - T_{Ci})\rho_i Cp_i - \left(\frac{UA_i}{V_{Ci}\rho_i Cp_i}\right)LMTD_i \tag{6}$$

Energy balances for the cooling fluid in *i*th heat exchanger:

$$\frac{d(T_{J_i})}{dt} = \frac{F_{J_i}}{V_{J_i}}(T_{J_e} - T_{J_i}) + \left(\frac{UA_i}{V_{J_i}\rho_J Cp_J}\right)LMTD_i \tag{7}$$

Logarithmic mean temperature difference (LMTD) for *i*th heat exchanger:

$$LMTD_i = \frac{(T_i - T_{J_i}) - (T_{Ci} - T_{J_e})}{\ln(T_i - T_{J_i})/(T_{Ci} - T_{J_e})} \tag{8}$$

where the subscripts i refer to each stage (fermentor); J_i and J_e are indexes referring to water inlet and outlet of the cooler; C is an index referring to

process fluid at the cooler; V (m^3) is the reactor volume; T (°C) is the temperature; F (m^3/h) is the flow rate; S (kg/m^3), X (g/L), and P (kg/m^3) are the substrate, cell, and ethanol concentrations, respectively; ρ (kg/m^3), Cp (J/kg·°C), and ΔH (J/kg) are density, specific heat, and reaction heat, respectively; and $Y_{X/S}$ and $Y_{P/S}$ are the kinetic parameters of yield. A kinetic model was validated with typical industrial conditions for this process *(14)*. The specific growth rate used was proposed by Lee et al. *(2)*:

$$\mu = \mu_{MAX} \frac{S}{K_S + S}\left(1 - \frac{P}{P_{MAX}}\right)^n \left(1 - \frac{X}{X_{MAX}}\right)^m \tag{9}$$

where μ_{MAX} (h^{-1}), P_{MAX} (kg/m^3), and X_{MAX} (kg/m^3) are the maximum specific growth rate, the product concentration when cell growth ceases and the biomass concentration when cell growth ceases, respectively, and n and m are inhibitor terms coefficients. The maximum specific growth rate, μ_{max}, is influenced by temperature and is calculated by the Arrhenius equation *(15)*:

$$\mu_{MAX} = Ae^{\frac{-E}{RT}} \tag{10}$$

According to Andrietta *(14)*, P_{MAX} has a constant value below a critical temperature (32°C) and above this temperature its value is described by:

$$P_{MAX} = K_0 e^{aT} \tag{11}$$

The kinetic parameters and constants used with Eqs. 1–11 are given by E = 6417 J/mol, $A = 4.5 \times 10^{10}$, $R = 8.314$ J/mol·K, $K_0 = 895.6$ kg/m^3, $a = -0.0676$ $°C^{-1}$, $X_{max} = 100$ kg/m^3, $n = 3.0$, $m = 0.9$, $K_s = 1.6$ kg/m^3, $Y_{P/S} = 0.445$, $Y_{X/S} = 0.033$ *(14)*. Table 1 shows the design parameters for the five fermentors.

The operations involved in the recycle (centrifuge, purge, dilution, and mixing) presents fast dynamics when compared with the fermentation process and can be considered in pseudo-steady-state. The concentrations of ethanol and substrate can be considered to remain constant in the value of the fermentor outlet at the centrifuge exit. Also, variations in density are considered negligible through the process. The equations are as follows:

$$F_W = \frac{F_0}{1 - RR} \tag{12}$$

$$F_R = F_W - F_0 \tag{13}$$

Cell concentration is kept constant in the recycle by manipulation of water flow rate, F_a. Mass balance on the dilution tank leads to:

$$F_{L1} = \frac{F_R X_R}{X_L} \tag{14}$$

Table 1
Design Parameters for the Five Fermentors

Reactor	A_i (m^2)	V (m^3)	F_c (m^3/h)	F_J (m^3/h)	V_c (m^3)	V_J (m^3)
1	76.361	433	400	400	20	20
2	63.242	370	350	350	20	20
3	31.061	366	180	180	20	20
4	6.809	359	60	60	20	20
5	2.869	333	28	30	20	20

$$F_a = F_R - F_{L1} \tag{15}$$

$$S_R = \frac{F_{L1} S_5}{F_R} \tag{16}$$

$$P_R = \frac{F_{L1} P_5}{F_R} \tag{17}$$

Mass balance on the centrifuge leads to:

$$F_V = F_W \frac{X_L - X_5}{X_L - X_V} \tag{18}$$

$$F_L = F_W - F_V \tag{19}$$

In the purge point we have:

$$F_S = F_L - F_{L1} \tag{20}$$

The concentrations of the first fermentor feeding are:

$$S_S = \frac{F_R S_R + F_0 S_0}{F_W} \tag{21}$$

$$P_W = \frac{F_R P_R}{F_W} \tag{22}$$

$$X_W = \frac{F_R X_R}{F_W} \tag{23}$$

The mathematical model is made by Eqs. 1–23 and solved using the fourth order Runge–Kutta method. The must feed flow rate used was $F_0 = 100$ m^3/h. Other parameters used in the equations are: $\Delta H = -6.509 \times 10^5$ J/kg, $\rho = 950$ kg/m^3, Cp = 4184.1 J/kg·°C, $U = 1.464 \times 10^7$ J/h·°C·m^2, $\rho_J = 1000$ kg/m^3, $Cp_J = 4184.1$ J/kg·°C *(14)*. The model does not consider cellular death because purge and recycle maintain the average age of cells in the process

from 7 to 10 d (young cells). Death rate is equal to the rate of cellular replacement and there is no accumulation of live cells or dead cells.

Hybrid Neural Model

The phenomenological model described by Eqs. 1–23 was determined by Andrietta *(14)* considering a real industrial process operating in continuous mode. It was validated with industrial data and shown to describe the process dynamic behavior accurately. However, this model is not able to describe the process in the presence of changes in operational conditions. In 2005, Andrietta evaluated this same model and concluded that, for the current operational conditions in the factory evaluated, the model of Ghose and Thyagi *(1)* with some modifications led to a better description of the process dynamic behavior. He also determined the existence of four groups of kinetic parameters in different harvesting periods in the year, which indicates that, in order to describe the dynamic behavior of the plant for long periods of time, the mathematical model should have its kinetic parameters updated periodically. However, the reestimation of kinetic parameters, mainly if they are considered functions of temperature, is a difficult and time-consuming task.

In order to solve this problem we used a hybrid neural model in which the kinetics is described by FLNs. The great advantage of these neural networks is that the estimation of its weights is a linear problem, and so the reestimation is rapid and convergence is guaranteed. The hybrid model consists of the mass and energy balance equations (Eqs. 1–8 and 12–23) and a FLN, which describes the specific biomass growth rate. The choice of this kinetic rate to be described by the neural network was made based on the results of a sensitivity analysis of the process.

Functional Link Networks

A neural network typically consists on many simple computational elements or nodes arranged in layers and operating in parallel. The weights, which define the strength of connection between the nodes, are estimated to yield good performance. Usually, in the training of neural networks, the inputs to a node are linearly weighted before the sum is passed through some nonlinear activation function that ultimately gives the network its nonlinear approximation ability. However, the same nonlinearity creates problems in learning the network weights, as nonlinear learning rules must be used, the learning rate is often unacceptably slow, and local minima may cause problems *(12)*. One way of avoiding nonlinear learning is the use of FLNs. In these networks, a nonlinear functional transformation or expansion of the network inputs is initially performed and the resulting terms are combined linearly. The obtained structure has a good nonlinear approximation capability and the estimation of the network weights is linear.

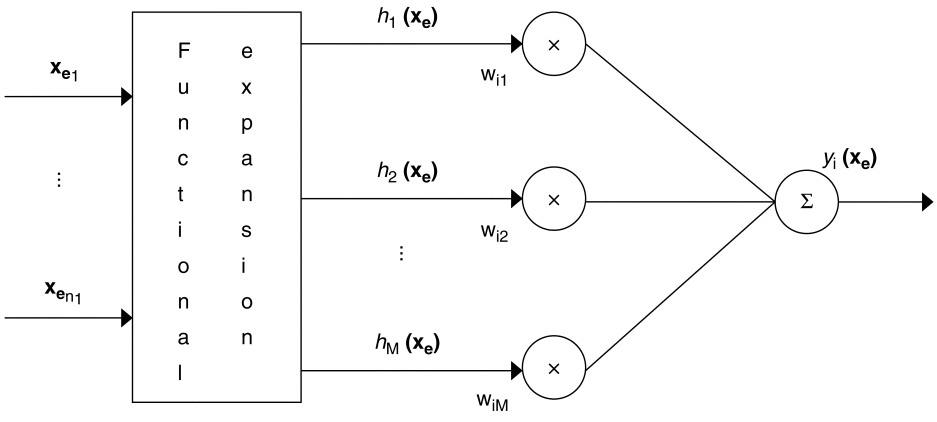

Fig. 2. General structure of a FLN.

The general structure of an FLN is shown in Fig. 2, where $\mathbf{x_e}$ is the input vector and $y_i(\mathbf{x_e})$ is an output. The hidden layer performs a functional expansion on the inputs, which maps the input space of dimension n_1, onto a new space of increased dimension, M ($M > n_1$). The output layer consists on m nodes, each one, in fact, a linear combiner. The input–output relationship of the FLN is

$$y_i(\mathbf{x_e}) = \sum_{J=1}^{M} w_{ij} h_J(\mathbf{x_e}), 1 < i \leq m \tag{24}$$

We use a modification in the structure of the FLNs, where the output given by Eq. 24 is transformed by an invertible nonlinear activation function. The new output is

$$y_i(\mathbf{x_e}) = f_i\left(\sum_{J=1}^{M} w_{ij} h_J(\mathbf{x_e})\right), 1 < i \leq m \tag{25}$$

where f_i is an invertible nonlinear function such as, for example, the sigmoidal function. Another modification in the FLNs used in this work is that the real inputs ($\mathbf{x_e}$) are transformed into a greater number (n_z) of auxiliary inputs ($\mathbf{z}$) before the functional expansion is performed. These modifications increase the nonlinear approximation ability of the network and yet, the estimation of the parameters remains a linear problem. A polynomial expansion of degree six is then performed on the new inputs. The generated monomials ($h_J[\mathbf{z}]$) are shown in Table 2.

Once the monomials are generated, the orthogonal least-squares estimator proposed by Billings et al. *(16)* is used to calculate the network weights (w_{ij}) and to eliminate the monomials, which are not significant in explaining the output variance. This reduces the size and complexity of the neural network and avoids overfitting of the data.

Table 2
Polynomial Expansion of Degree Six

Degree	Monomials
0	1
1	z_i ($i = 1, n_z$)
2	$z_i z_j$ ($i = 1, n_z, j = i, n_z$)
3	$z_i z_j z_k$ ($i = 1, n_z, j = i, n_z$, and $k = j, n_z$)
4	$z_i z_j z_k z_l$ ($i = 1, n_z, j = i, n_z, k = j, n_z$, and $l = k, n_z$)
5	$z_i z_j z_k z_l z_m$ ($i = 1, n_z, j = i, n_z, k = j, n_z, l = k, n_z$, and $m = l, n_z$)
6	$z_i z_j z_k z_l z_m z_n$ ($i = 1, n_z, j = i, n_z, k = j, n_z$, $l = k, n_z, m = l, n_z$, and $n = m, n_z$)

Table 3
Full Factorial Design With Axial Points
and One Center Point

Time (h)	S_0 (g/L)	T_0 (°C)
10	158.8	29
20	158.8	34
30	201.2	29
40	201.2	34
50	150	31.5
60	210	31.5
70	180	28
80	180	35
90	180	31.5

Training of the Neural Network

The network inputs ($\mathbf{x_e}$) are the process state variables: biomass, substrate and product concentrations, and temperature. The output is the specific growth rate. In this work, the state variables are considered accessible by direct measurement, but the output is not measurable. It can be estimated from measured experimental data by the discretization of the biomass balance equation. When dealing with noisy data, some kind of smoothing algorithm has to be applied to produce reliable rate values from biomass concentration data. Training was performed using a full factorial design, considering axial points and one center point, involving the variables S_0 and T_0. Both variables had their values changed every 10 h within the ranges 150–210 g/L (S_0) and 28–35°C (T_0). Ten hours is enough time for the process to reach a new steady state. Table 3 shows the factorial design.

During training and validation the performance of the FLN was measured by Eq. 26, given by Milton and Arnold *(17)*:

$$\text{cor} = \left(1 - \frac{\sum_{k=1}^{N} [y_e(k) - y(k)]^2}{\sum_{k=1}^{N} [y_e(k) - \overline{y}_e]^2} \right) 100\% \tag{26}$$

where $y_e(k)$ is the real output, $y(k)$ is the network output, $\overline{y}_e$ is the mean value of the real outputs and N is the number of training points. For validation, the disturbances encompassed a sequence of steps with random changes every 10 h within the ranges 162–198 g/L (S_0) and 28°C to 32°C (T_0). During training and validation the activation function that led to the best performance is given by Eq. 27:

$$f\left(\sum_{J=1}^{M} w_{ij} h_j(\mathbf{z}) \right) = \frac{1}{\sum_{J=1}^{M} w_{ij} h_j(\mathbf{z})} \tag{27}$$

The auxiliary input vectors were chosen for each reactor after many tests and are given in Table 4.

Results

For the five process fermentors, the best performance of the FLNs was obtained using fifth degree monomials. Using four auxiliary inputs (as shown in Table 4) we generated 126 monomials for each of the five FLNs (each one describing the specific growth rate of one fermentor). After using the orthogonal least-squares estimator proposed by Billings et al. *(16)* to eliminate nonsignificant monomials, the number of monomials for each network was drastically reduced, as can be seen in Table 5, which shows the number of monomials and the performance of the five FLNs during validation (measured by Eq. 26).

The number of monomials in the FLNs can be considered equivalent to the number of connections (or weights) in a multilayer perceptron neural network.

The five FLNs are described by Eqs. 28–32:

$$\mu_{\text{FLN}}(\text{Fermentor 1}) = \frac{1}{-1.4295 T^{1.18} + 1.1165 \times 10^{-23} X^{6.04} \frac{1}{S} P^{9.84} + 6.8689 \times 10^{-7} X^{6.04} P^{4.92} T^{1.18}} \frac{1}{-5.0705 \times 10^{-13} X^{3.02} P^{4.92} T^{1.77} + 7.5585 \times 10^{-7} X^{3.02} T^{2.36} - 5.104 \times 10^{-24} \frac{1}{S} P^{14.76} T^{0.59}} \frac{1}{+9.7211 \times 10^{-10} P^{4.92} T^{2.36}} \tag{28}$$

Table 4
Input Vectors of the Network

Reactor	Vector (**z**)
1	$z = \left[X^{3.02} \frac{1}{S} P^{4.92} T^{0.59} \right.$
2	$z = \left[X^{2.7} \frac{1}{S} \frac{1}{P^{4.0}} T^{0.6} \right]$
3	$z = \left[X^{3.0} \frac{1}{S} P^{4.90} T \right]$
4	$z = \left[X \frac{1}{S} P T^{0.4} \right]$
5	$z = \left[X^{1.25} \frac{1}{S} P T^{0.59} \right]$

Table 5
Performance and Number of Monomials for the FLN

Reactor	Number of monomials	Performance (%)
1	7	99.6870
2	6	99.6868
3	11	99.9895
4	18	99.7873
5	18	96.6931

$$\mu_{\mathrm{FLN}}(\mathrm{Fermentor\,2}) = \frac{1}{-334.11 + 0.0060987 X^{8.1} \frac{1}{P^{4.0}} + 1.1656 \times 10^{-14} X^{10.8} \frac{1}{S} - 7.2676 \times 10^{-7} X^{10.8} \frac{1}{P^{4.0}} \frac{1}{-4.5488 \times 10^{-11} X^{8.1} \frac{1}{S^{2.0}} + 8.6769 \times 10^{-9} X^{5.4} T^{1.8}}} \tag{29}$$

$$\mu_{\mathrm{FLN}}(\mathrm{Fermentor\,3}) = \frac{1}{9039.3 - 323.37T - 0.00033194 \frac{1}{S} P^{4.9} + 3.0911 \times 10^{-5} \frac{1}{S} P^{4.9} T - 9.6048 \times 10^{-7} \frac{1}{S} P^{4.9} T^2 \frac{1}{-8.9072 \times 10^{-11} P^{4.9} T^{3.0} - 5.2582 \times 10^{-11} X^{6.0} T^{3.0} + 9.2656 \times 10^{-8} X^{3.0} T^{4.0} \frac{1}{+2.7862 \times 10^{-5} \frac{1}{S^{3.0}} T^{2.0} + 9.9624 \times 10^{-9} \frac{1}{S} P^{4.9} T^{3.0} + 2.8483 \times 10^{-12} P^{4.9} T^{4.0}}} \tag{30}$$

$$\mu_{FLN\,(Fermentor\,4)} = \frac{1}{-2899.6 - 0.53749X\frac{1}{S^{2.0}}P + 0.27431\frac{1}{S^{2.0}}P^{2.0} - 0.017078\frac{1}{S}P^{3.0} + 2.0252PT^{1.2}}$$
$$\frac{1}{-2.3187\times10^{-6}X\frac{1}{S^{4.0}} - 0.0053256X\frac{1}{S^{2.0}}P^{2.0} + 0.21679X\frac{1}{S^{2.0}}PT^{0.4}}$$
$$\frac{1}{-0.043293XPT^{1.2} + 1.6239\times10^{-9}\frac{1}{S^{5.0}} + 1.8985\times10^{-7}\frac{1}{S^{4.0}}P + 1.5343\times10^{-5}\frac{1}{S^{4.0}}T^{0.4}} \quad (31)$$
$$\frac{1}{-3.8448\times10^{-7}\frac{1}{S^{3.0}}P^{2.0} + 0.0010677\frac{1}{S^{2.0}}P^{3.0} - 0.072847\frac{1}{S^{2.0}}P^{2.0}T^{0.4}}$$
$$\frac{1}{-2.9298\frac{1}{S^{2.0}}T^{1.2} + 2.3907\times10^{-5}\frac{1}{S}P^{4.0} + 0.0039741\frac{1}{S}P^{3.0}T^{0.4}}$$

$$\mu_{FLN\,(Fermentor\,5)} = \frac{1}{-7511.3\frac{1}{S} - 0.0046055\frac{1}{S^{2.0}}P + 10.992\frac{1}{S}P^{2.0} + 13.016T^{1.77} - 9.8779\times10^{-9}\frac{1}{S^{4.0}}}$$
$$\frac{1}{-0.23645\frac{1}{S}P^{3.0} - 0.00058067X^{3.75}\frac{1}{S^{2.0}} + 0.01669X^{2.5}\frac{1}{S^{2.0}}T^{0.59}}$$
$$\frac{1}{-0.15954X^{1.25}\frac{1}{S^{2.0}}T^{1.18} - 0.019771X^{1.25}T^{2.36} - 1.1657\times10^{-14}\frac{1}{S^{5.0}}} \quad (32)$$
$$\frac{1}{+1.3446\times10^{-9}\frac{1}{S^{4.0}}T^{0.59} + 5.2132\times10^{-9}\frac{1}{S^{3.0}}P^{2.0} - 7.4404\times10^{-8}\frac{1}{S^{3.0}}PT^{0.59}}$$
$$\frac{1}{+1.8348\times10^{-7}\frac{1}{S^{3.0}}T^{1.18} + 0.50787\frac{1}{S^{2.0}}T^{1.77} + 0.0013531\frac{1}{S}P^{4.0}}$$
$$\frac{1}{+0.0009187\frac{1}{S}P^{3.0}T^{0.59}}$$

The quality of prediction of the proposed hybrid neural model was measured by the residual standard deviation (RSD) described as a percentage of average of the 'real' values, as described by Atala et al. *(3)*:

$$\mathrm{RSD}(\%) = \frac{\mathrm{RSD}}{\overline{Y}_i}\times100 \quad (33)$$

$$\mathrm{RSD} = \frac{\sqrt{\sum_{i=1}^{n}\left(y_i - y_{Pi}\right)^2}}{n} \quad (34)$$

In this equation y_i is the "real" value (calculated by the deterministic model), y_{Pi} is the value predicted by the hybrid model and n is the number

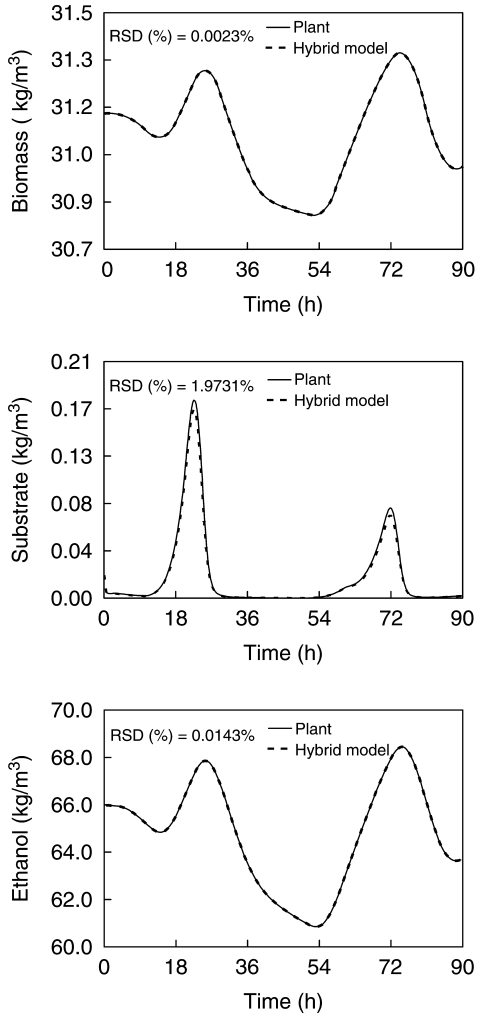

Fig. 3. Concentrations of biomass, substrate, and product in the fifth fermentor (deterministic model —, hybrid model).

of points. Figure 3 shows the performance of the hybrid model to describe the dynamic behavior of the fifth fermentor when the process is subjected to the disturbances shown in Fig. 4. In this figure the disturbances performed for training of the neural networks are shown for comparison. Table 6 shows the values of RSD% obtained when we use the mathematical model to calculate concentrations of biomass, substrate, and product in the five fermentors. If a model without update of its parameters is used it is not possible to obtain good predictions, and errors over 50% might be found depending on the type and level of changes.

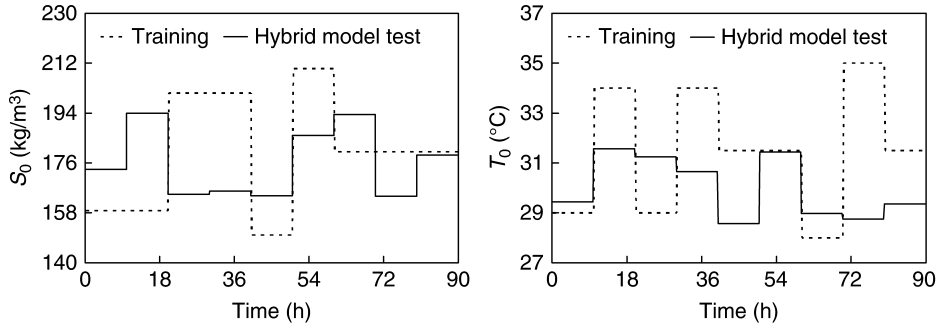

Fig. 4. Disturbances for the test of the hybrid model.

Table 6
Model Quality of Prediction Described by the RSD (%)

Reactor	Biomass X (kg/m^3)	Substrate S (kg/m^3)	Product P (kg/m^3)
1	0.0037	0.1506	0.0323
2	0.0021	0.3097	0.0147
3	0.0020	0.7540	0.0126
4	0.0024	1.4294	0.0149
5	0.0023	1.9731	0.0143

Discussion

Bioreactors are quite difficult to model because their operation involves microbial growth under constantly changing conditions. Past experience has shown the difficulties of using phenomenological models without kinetic parameters reestimation to describe the dynamic behavior of the process for long periods of operation, when there are changes in substrate and yeast conditions (a common situation in industrial plants). However, the reestimation of kinetic parameters in a phenomenological model is difficult and time-consuming, mainly when the kinetics dependence on temperature is taken into account. As the main nonlinearities and uncertainties are in the description of the process kinetic, the use of a hybrid approach whereby the kinetics is described by a FLN can simplify the reestimation step.

In this work, we have shown that a hybrid neural model combining mass balance equations with FLNs is able to describe the process dynamic behavior with a performance similar to that of a phenomenological model. However, the reestimation of the weights of a FLN is much simpler than the reestimation of kinetic parameters in a phenomenological model. The estimation of the FLN weights is a linear optimization problem, so it is very fast and convergence is guaranteed. The use of this approach enables the development of an online reestimation procedure.

Conclusions

The proposed hybrid model seems to be a quite suitable approach to follow changes in the process that impact the system behavior. The reestimation of the hybrid model is easily done especially because the model is built-up using FLNs. These networks showed to have a good nonlinear approximation capability, although the estimation of its weights is linear. The proposed approach for hybrid modeling is able to deal with disturbances in transient phases of the process and different yeasts, because the identification procedures is carried out adequately with an appropriate set of data representative of the biotechnological process.

Acknowledgments

The authors acknowledge Fundação de Amparo à Pesquisa do Estado de São Paulo (FAPESP) and Conselho Nacional de Desenvolvimento Científico e Tecnológico (CNPq) for financial support.

Nomenclature

a	constant in Eq. 11
A	constant in Eq. 10
A_i	area of the ith heat exchanger (m^2)
Cp	reagent fluid heat capacity (J/kg·°C)
Cp_J	cooling fluid heat capacity (J/kg·°C)
E	activation energy (J/mol)
f	activation function of the FLN
F_a	water flow rate (m^3/h)
F_{Ci}	reagent fluid flow rate to the ith heat exchanger (m^3/h)
F_i	feed stream flow rate to ith reactor (m^3/h)
F_{Ji}	cooling fluid flow rate in the ith heat exchanger (m^3/h)
F_L	cell suspension flow from centrifuge (m^3/h)
F_{L1}	cell suspension flow to treatment tank (m^3/h)
F_0	fresh medium flow rate (m^3/h)
F_R	cell recycling flow rate (m^3/h)
F_S	purge flow rate (m^3/h)
F_V	liquid-phase flow to rectification column (m^3/h)
F_W	feed stream flow rate (m^3/h)
h	monomials generated by the functional expansion
K_0	constant in Eq. 11
K_s	substrate saturation constant (kg/m^3)
$LMTD_i$	logarithmic mean temperature difference for the ith heat exchanger
m	constant in Eq. 9
m	number of outputs of the FLN

M	number of monomials
n	constant in Eq. 9
n_z	number of auxiliary inputs
P_i	product concentration in the *i*th reactor (kg/m^3)
P_{MAX}	product concentration when cell growth ceases (kg/m^3)
P_R	product concentration in the cells recycle (kg/m^3)
P_W	feed product concentration (kg/m^3)
R	universal gas constant (J/mol·K)
RR	cell recycle rate
S_i	substrate concentration in the *i*th reactor (kg/m^3)
S_0	inlet substrate concentration (kg/m^3)
S_R	substrate concentration in the cells recycle (kg/m^3)
S_W	feed substrate concentration (kg/m^3)
t	time (h)
T_{Ci}	temperature of the reagent fluid in the *i*th heat exchanger (°C)
T_i	temperature in the *i*th reactor (°C)
T_{Ji}	cooling fluid temperature at the *i*th heat exchanger exit (°C)
T_{Je}	inlet cooling fluid temperature in the *i*th heat exchanger (°C)
U	global exchange coefficient (J/h·°C·m^2)
V_i	volume of the *i*th reactor (m^3)
V_{Ji}	cooling fluid volume in the *i*th heat exchanger (m^3)
w	FLN weights
$\mathbf{x_e}$	input vector of the FLN
X_i	biomass concentration in the *i*th reactor (kg/m^3)
X_L	biomass concentration in the heavy phase from centrifuge (kg/m^3)
X_{MAX}	biomass concentration when cell growth ceases (kg/m^3)
X_R	cell recycling concentration (kg/m^3)
X_V	biomass concentration in the light phase to rectification column (kg/m^3)
X_W	feed biomass concentration (kg/m^3)
$Y_{P/S}$	yield of product based on cell growth (kg/kg)
$Y_{X/S}$	limit cellular yield (kg/kg)
$\mathbf{z}$	auxiliary input vector

Greek letters

ΔH	reaction heat (J/kg)
ρ_i	reagent fluid density in the *i*th reactor (kg/m^3)
ρ_j	cooling fluid density (kg/m^3)
μ_i	specific growth rate in the *i*th reactor (h^{-1})
μ_{MAX}	maximum specific growth rate (h^{-1})

References

1. Ghose, T. K. and Tyagi, R. D. (1979), *Biotechnol. Bioeng*. **21,** 1387–1400.
2. Lee, J. M., Pollard, J. F., and Coulman, G. A. (1983), *Biotechnol. Bioeng*. **25,** 497–511.

3. Atala, D. I. P., Costa, A. C., Maciel Filho, R., and Maugeri Filho, F. (2001), *Appl. Biochem. Biotech.* **91(3),** 353–365.
4. Aldiguier, A. S., Alfenor, S., Cameleyre, X., et al. (2004), *Bioproc. Biosyst. Eng.* **26,** 217–222.
5. Costa, A. C., Alves, T. L. M., Henriques, A. W. S., Maciel Filho, R., and Lima, E. L. (1998), *Comput. Chem. Eng.* **22,** 859–862.
6. Harada, L. H. P., Costa, A. C., and Maciel Filho, R. (2002), *Appl. Biochem. Biotech.* **98(1–9),** 1009–1024.
7. Psichogios, D. C. and Ungar, L. H. (1992), *AIChE J.* **38,** 1499–1511.
8. Smets, I. Y., Claes, J. E., November, E. J., Bastin, G. P., and Van Impe, J. F. (2004), *J. Proc. Control* **14,** 795–805.
9. Nishiwaki, A. and Dunn, I. J. (1999), *Biochem. Eng. J.* **4,** 37–44.
10. Ricci, M., Martini, S., Bonechi, C., Trabalzini, L., Santucci, A., and Rossi, C. (2004), *Chem. Phys. Lett.* **387,** 377–382.
11. Patnaik, P. R. (2003), *Biochem. Eng. J.* **15,** 165–175.
12. Chen, S. and Billings, S. A. (1992), *Int. J. Control* **56,** 319–346.
13. Andrietta, S. R. and Maugeri, F. (1994), *Adv. Bioprocess Eng.* **1,** 47–52.
14. Andrietta, S. R. (1994), *PhD Thesis*, State University of Campinas, SP, Brazil.
15. Fogler, H. S. (1999), *Elements of Chemical Reaction Engineering*, 3rd ed. Prentice Hall, New York.
16. Billings, S. A., Chen, S., and Korenberg, M. J. (1989), *Int. J. Control* **49,** 2157–2189.
17. Milton, J. S. and Arnold, J. C. (1990), *Introduction to Probability and Statistics*, McGraw Hill, New York.